PETROVIETNAM JOURNAL
Volume 6/2020, pp. 30 - 36
ISSN 2615-9902

CALCULATING PRECISE WATER SATURATION WITH HYDRAULIC FLOW UNIT USING LEVERETT'S J-FUNCTION. A CASE STUDY OF FIELD A, CUU LONG BASIN, OFFSHORE VIETNAM

Phung Van Phong, Pham Thi Hong, Vu The Anh
Vietnam Petroleum Institute (VPI)
Email: phongpv@vpi.pvn.vn

Summary

Estimating water saturation is one of the main challenging aspects in reservoir characterisation. Good estimation of this parameter enables us to calculate reserve accurately. Hence, it is of great importance to estimate precisely water saturation based on hydraulic flow units of reservoir rocks. In this paper, a modified J-function was used and developed to determine the water saturation in the hydrocarbon reservoirs located in field A, Cuu Long basin. The capillary pressure data (P_c) and water saturation (S_w) as well as routine core sample analysis including porosity (φ) and permeability (K) were used to develop the J-function. First, the normalised porosity (Φ_z), the rock quality index (RQI), and the flow zone indicator (FZI) factors were used to classify all data into discrete hydraulic flow units (HU) containing unique pore geometry and bedding characteristics. Subsequently, the modified J-function was used to normalise all capillary pressure curves corresponding to each of predetermined HUs. The results showed that the reservoir rock was classified into several separate rock types with definite HUs and reservoir pore geometry. Eventually, the water saturation was determined using a developed equation corresponding to each HU gained by normalised J-function. The equation is a function of rock characteristics including Φ_z, FZI, lithology (J'), and pore size distribution index (∂). The proposed technique can be applied to any reservoir to determine the water saturation in the reservoir, specially the ones with high range of heterogeneity in the reservoir rock properties.

Key words: Water saturation, rock quality index (RQI), hydraulic unit (HU), flow zone index (FZI), Cuu Long basin.

1. Introduction

Flow regime of fluid and accurate water saturation are among the challenges in hydrocarbon reservoir studies and extremely affected by the geometry of pore size in the reservoir. The results of diagenesis such as compaction, cementation, oxidation and fracturing through geological times will create irregular pore geometry. To precisely determine water saturation of the reservoir rocks, a robust model is proposed to simulate the flow behaviour in the reservoir. Up to now, there are numerous approaches to determine water saturation. Among them, capillary pressure curves are used more commonly because of their direct relation to water level with each pore size throat and distribution in reservoir rock. The capillary pressure is expressed as the difference in pressure between the non-wetting (P_{nw}) and wetting (P_w) phases as in Equation (1).

$$P_c = P_{nw} - P_w \quad (1)$$

If oil and water are present in the reservoir, Equation (1) can be written as Equation (2).

$$P_{cow} = P_o - P_w \quad (2)$$

Moreover, the capillary pressure is also a function of the interaction between rocks and fluids. It is affected by several factors of rock such as pore geometry, r-pore radius (pore size), γ-interfacial tension and wettability with θ being the contact angle as in Equation (3):

$$P_c = \frac{2\gamma cos\ \theta}{r} \quad (3)$$

Normally, a reservoir consists of many intervals with different properties or heterogeneity. Each interval is reflected by a specific shape of the capillary pressure curve that reveals useful information about reservoir rock property. And because of the heterogeneity existing commonly in the reservoir rocks, no single capillary pressure curve can be considered as a representative of the reservoir. Therefore, the capillary pressure curves need to be nor-

Date of receipt: 19/2/2019. Date of review and editing: 19/2/2019 - 9/3/2020.
Date of approval: 5/6/2020.

malised into a single curve using a Leverett dimensionless J-function [1] for a unique rock type with RQI known as rock quality index and defined by the square of permeability and porosity of rock as follows:

$$J(S_w) = \frac{P_C}{\gamma\, cos\theta}\sqrt{\frac{k}{\varphi}} \quad (4)$$

$$J(S_w) = \frac{P_C}{\gamma\, cos\theta}\, RQI \quad (5)$$

According to Equation (5), the normalised J-function can be applied to a single rock type with uniform rock properties (RQI).

2. Theory overview

To determine hydraulic units and allows(?) a suitable relationship among porosity, permeability, capillary pressure and geological variation in the reservoir rock, the mean hydraulic unit radius (r_{mh}) need to be determined and can be defined by the ratio of cross-sectional area to wetted perimeter as in Equation (6) [2]:

$$r_{mh} = \frac{\pi r^2}{2\pi r} = \frac{r}{2} \quad (6)$$

According to Darcy's and Poiseuille's Laws, a relationship between porosity and permeability can be derived as shown in Equation (7) with φ and τ representing porosity and tortuosity, respectively [2].

$$k = \frac{r^2\varphi}{8\tau^2} \quad (7)$$

The relationship between rock porosity and permeability depends on both geometrical characteristics of pore size (radius) and pore shape. Combining Equations (6) and (7), the permeability can be re-written as Equation (8):

$$k = \frac{r^2\varphi}{8\tau^2} = \frac{\varphi}{2\tau^2}\left(\frac{r}{2}\right)^2 = \frac{\varphi, r_{mh}^2}{2\tau^2} \quad (8)$$

The mean hydraulic radius in terms of surface area per unit grain volume (S_{gv}) and porosity can be expressed by:

$$r_{mh} = \frac{1}{S_{gv}}\left[\frac{\varphi}{1-\varphi}\right] \quad (9)$$

According to Equations (8) and (9), substituting r_{mh} into the Kozeny and Carmen relationship from Equation (8), the rock permeability can be presented as follows:

$$k = \frac{\varphi 3}{(1-\varphi)2}\left[\frac{1}{\tau^2 S_{gv}^2}\right] \quad (10)$$

Dividing both sides of Equation (10) by the porosity and then taking square root, the equation can be re-written as follows:

$$\sqrt{\frac{k}{\varphi}} = \frac{\varphi}{1-\varphi}\left[\frac{1}{1.14\tau S_{gv}}\right] \quad (11)$$

As mentioned in Equations (4) and (5), the normalised porosity as $\varphi_z = \left(\frac{\varphi}{1-\varphi}\right)$ and flow zone indicator (FZI) as $FZI = \frac{1}{1.14\tau S_{gv}}$, Equation (11) can be re-organised as follows [3]:

$$RQI = \phi_z \times FZI \quad (12)$$

Flow zone indicator is a unique and valuable factor to quantify the fluid flow in a reservoir and is the one that displays the relationship of petrophysical properties.

Finally, using a unique J-function can normalise capillary pressure curves into a single curve for a definite hydraulic flow unit as in Equation (13) [4, 5]:

$$J(S_w) = \frac{P_c}{\gamma cos\theta}\varphi_z \times FZI \quad (13)$$

Re-writing Equation (3) gives:

$$\frac{P_C}{\gamma cos\theta} = \frac{2}{r} \quad (14)$$

By substituting Equation (14) into Equation (13), one can derive:

$$J(S_w) = \frac{2}{r}\varphi_z \times FZI \quad (15)$$

For a single hydraulic flow unit with unique FZI value, the J-function can be written as follows with J′ and ∂ representing lithology and pore size distribution index, respectively [5]:

$$J(S_w) = J' \times S_{wn}^{\frac{-1}{\partial}} \quad (16)$$

Where:

$$S_{wn} = \frac{s_w - s_{wir}}{1 - s_{wir}} \quad (17)$$

According to Equations (16) and (17), water saturation in the reservoir can be calculated by a function of normalised water saturation, irreducible water saturation and J-function for each hydraulic flow unit.

3. Regional setting and reservoir property

The study area is located in the Cuu Long basin. The basin is an Early Tertiary rift basin situated off the southeast coast of Vietnam. Geo-dynamic processes and environments dominate the offshore basin evolution related to plate tectonic events, such as: northern collision of India with Asia ~53Ma ago and related extrusion tectonics until the present day; escape tectonics of the Indochina Block; the Philippine trench roll back; the opening of the East Sea/Bien Dong (Late Oligocene - Early Miocene); the northern collision of the Australian plate with Southern Sunda land Indochina and its offshore basins; NW-SE

opening of the basin began in Late Eocene(?) Oligocene time; the opening of the basin is related to crustal stretching associated with the clockwise rotation of Indochina; the basin is located at the trailing edge of the Wang Chao/ Hau River fault system, which currently controls the position of the Mekong delta; the basin and the neighbouring Nam Con Son basin are separated by the Con Son swell, a transgressional feature potentially linked to the NS trending 'Vietnam Transform'; the 'Vietnam Transform' defines the present shelf break offshore Vietnam. It 'accommodates' the deformation along the eastern boundary of the Indochina block. Thus, coeval NW-SE extension and NS shearing are reckoned to occur during the Cuu Long basin opening.

The study interval was formed in fluvial to lacustrine environments with some interbedded sandstone and claystone based on the detailed facies, grain size and petrographic analysis of the cores. In terms of reservoir properties, log and core data show that reservoir cementation is in advanced stages, especially in the deeper parts of the reservoir. Some core thin sections indicate good visible primary porosity while most others have complete primary porosity occlusion. And most of the thin sections contain some amount of secondary porosity, bringing to light the importance of distinguishing measured porosity from connected porosity.

Most of the sandstones contain a large amount of cement and authigenic minerals. The main authigenic minerals observed in SEM analysis include quartz, diagenetic clays, zeolite (laumontite), albite and calcite. Quartz cement is present in common to very abundant amounts in all examined sandstones. It occurs mostly as euhedral crystals (from 5 mm – 10 mm to more than 100 mm in length) that are surrounded by detrital quartz grains and/ or occluding intergranular pores and pore throats. The strong development of quartz cement is one of the main factors that strongly reduces both primary intergranular porosity and permeability of all sandstones at the interval. Moreover, the authigenic clays consist mainly of illite and chlorite with minor kaolinite. These clays occur mainly as uniform mats coating detrital grains and to a lesser extent as feldspar and mica grains replacement. Locally, authigenic illite occurs as thin ribbons, or short fibres/webs occluding and bridging pore spaces. It is likely that this kind of illite morphology causes permeability barriers that inhibit pore-fluid flow, i.e. it severely reduces the permeability of these sandstones. Additionally, the laumontite cement is present in minor to common amounts and occurs mostly as large, euhedral, tabular crystals more than 50 mm long. These mainly fill intergranular pores and/or partly replace detrital feldspar grains. The moderate to strong development of laumontite in some samples

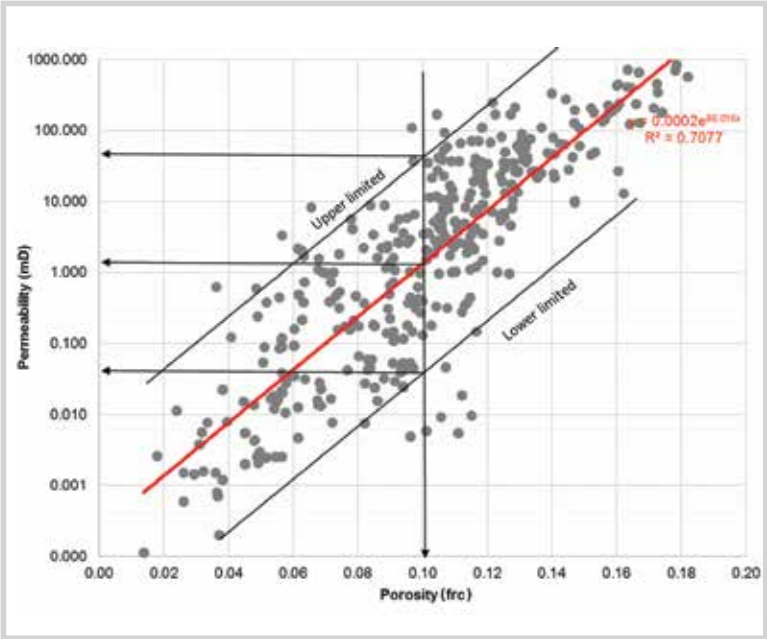

Figure 1. *The relationship of permeability and porosity in the reservoir according to core sample analysis*

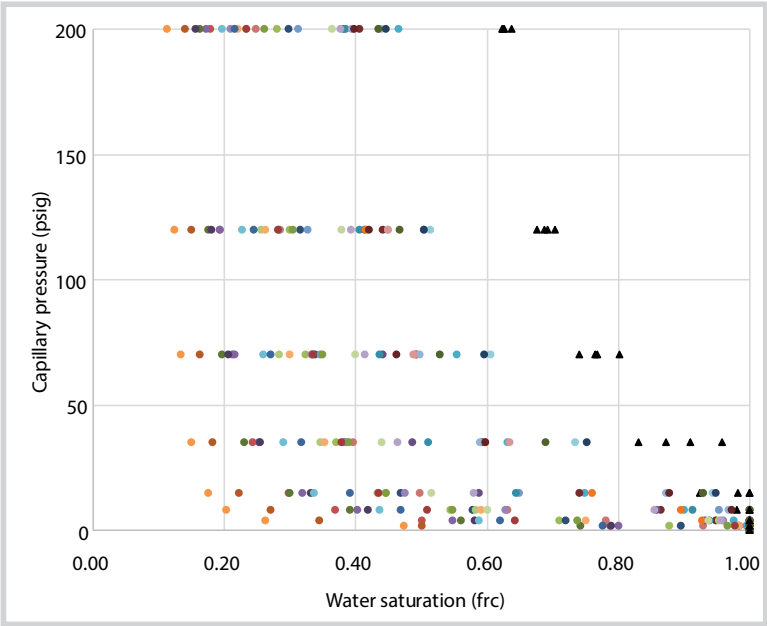

Figure 2. *Distribution of capillary pressure curves of 60 reservoir rock samples.*

considerably reduces intergranular porosity. Calcite cement is generally minor and occurs mainly as sparry crystals filling intergranular pores. Secondary albite is present in minor amounts and often occurs as fine, subhedral to euhedral crystals of 5 mm to more than 20 mm. They are often surrounded partly by detrital feldspar grains.

4. Database and methodology

Database is used to complete the study including porosity (φ), permeability (k), irreducible water saturation (S_{wir}) and capillary pressure (P_c) vs. water saturation (S_w) obtained from core analyses in the Cuu Long basin. The huge PVT result from 485 routine core data and 60 complete data sets of capillary pressure measured by porous disk method are analysed. Figure 1 shows a large permeability and porosity variation of all reservoir core data. As shown in this figure, there is a high heterogeneity in the reservoir rock properties. For example, given the same value of porosity, the permeability could be changing up to 100 times. The statistical data of 60 core samples with a complete data set are dis-

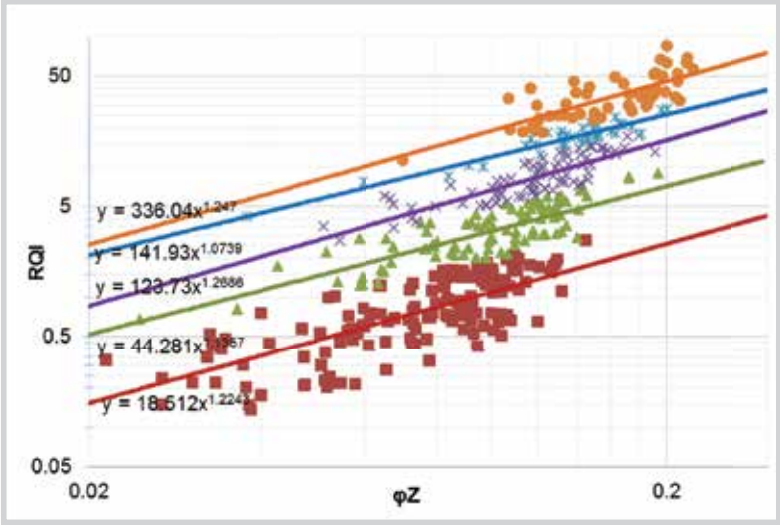

Figure 3. *Relationship of reservoir quality index (RQI) and normalised porosity in field A.*

Table 1. *Rock properties of 60 samples taken from the capillary pressure curves*

Sample No.	Permeability (K), md	Porosity (φ)	S_{wir}	Sample No.	Permeability (K), md	Porosity (φ)	S_{wir}
1	0.04	0.08	0.62	31	1.75	0.08	0.26
2	192.80	0.16	0.18	32	2.66	0.11	0.31
3	8.19	0.13	0.28	33	2.49	0.10	0.35
4	50.37	0.15	0.17	34	2.24	0.08	0.35
5	0.32	0.11	0.46	35	0.22	0.09	0.56
6	708.77	0.18	0.11	36	0.34	0.10	0.52
7	3.49	0.08	0.30	37	0.50	0.09	0.48
8	0.47	0.08	0.41	38	5.50	0.11	0.32
9	40.04	0.13	0.16	39	0.15	0.08	0.59
10	37.29	0.10	0.16	40	0.71	0.10	0.38
11	0.05	0.05	0.62	41	0.68	0.09	0.39
12	340.42	0.14	0.14	42	0.47	0.10	0.39
13	670.00	0.17	0.14	43	0.36	0.09	0.39
14	418.00	0.17	0.16	44	0.20	0.09	0.43
15	259.00	0.16	0.17	45	3.38	0.09	0.36
16	0.03	0.07	0.80	46	1.06	0.08	0.38
17	0.63	0.10	0.66	47	0.11	0.08	0.44
18	29.40	0.13	0.31	48	0.29	0.12	0.50
19	64.00	0.13	0.25	49	2.32	0.12	0.41
20	79.60	0.13	0.25	50	0.14	0.10	0.46
21	11.80	0.12	0.27	51	0.30	0.10	0.44
22	4.45	0.12	0.31	52	0.15	0.10	0.46
23	0.16	0.06	0.31	53	0.90	0.11	0.40
24	1.07	0.07	0.25	54	6.72	0.11	0.35
25	0.98	0.07	0.23	55	0.67	0.11	0.44
26	0.70	0.07	0.21	56	0.66	0.10	0.41
27	4.30	0.08	0.20	57	0.04	0.06	0.64
28	3.71	0.10	0.22	58	0.09	0.07	0.45
29	4.46	0.09	0.22	59	0.30	0.08	0.40
30	1.66	0.07	0.23	60	0.17	0.08	0.43

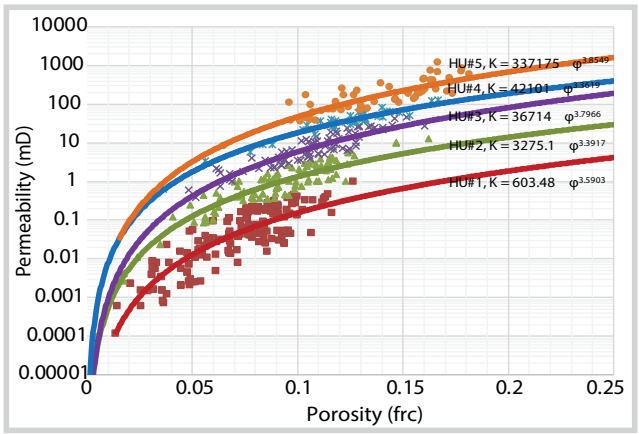

Figure 4. *Permeability and porosity distribution with FZI classified in field A.*

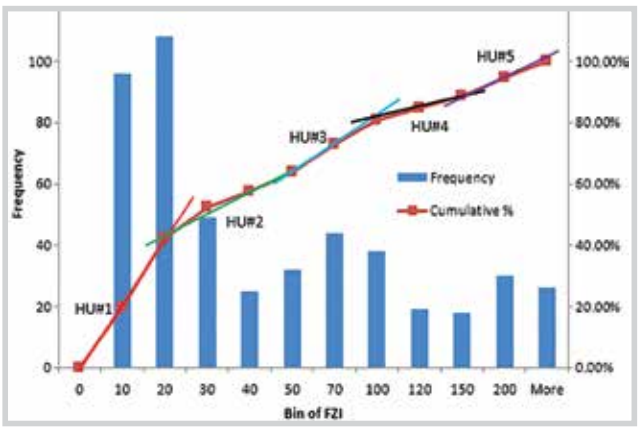

Figure 5. *Frequency of FZI to define HU in field A.*

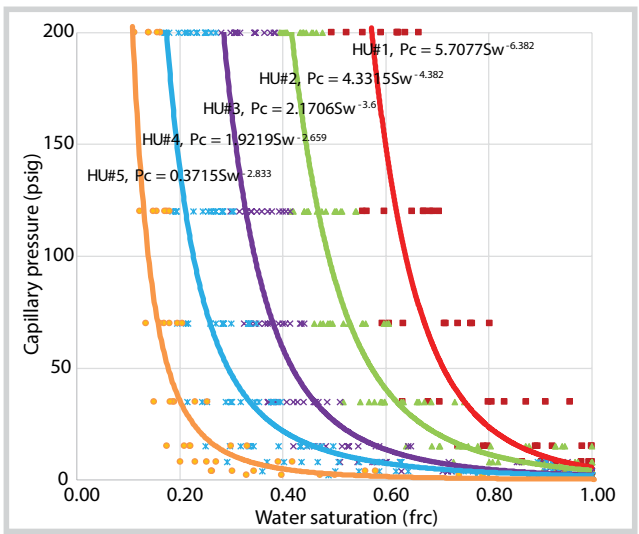

Figure 6. *Five capillary pressure data sets for obtained hydraulic flow units in Field A.*

played in Table 1. Figure 2 demonstrates the measured capillary pressure curves and water saturation. This figure reveals that more than one hydraulic flow unit in the reservoir can be observed clearly. Therefore, the J-function cannot be used to normalise all the capillary data into a single curve and it is required to classify the data into separate hydraulic flow units having the same type of capillary pressure curves.

According to the data shown, irreducible water saturation broadly varies from 0.15 up to 0.65 depending on the sample properties.

5. Results and discussions

After rock quality index (RQI) and normalised porosity (ϕ_z) are estimated by the equations mentioned above, the results are plotted together in Figure 3. Commonly, all data are in correlation with unit slope having the same mean value of FZI factor. Based on the data and Figure 3, several hydraulic flow units such as HU#1, HU#2, HU#3, HU#4 and HU#5 can be defined as separate rock types with the mean values of FZI being 10.7, 33.1, 71.1, 123.1 and 220.8, respectively. It is clear that hydraulic flow units with higher FZI values will have a faster flow of the fluids in the reservoir.

Figure 4 illustrates the relationships of the permeability and porosity grouping by FZI category (Figure 5). With

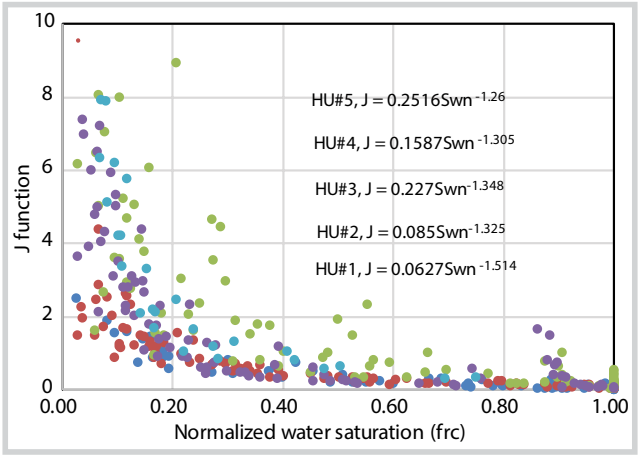

Figure 7. *J-function and normalised water saturation for each hydraulic flow unit.*

Table 2. *Rock characteristics and equations obtained for each hydraulic flow unit*

	FZI-mean	J'	∂	Permeability Equation	Normalised J-function Equation	Pore size radius Equation
HU#1	10.7	0.063	0.660502	K = 603.48φ3.5903	J = 0.0627 × $S_{wn}^{-1.514}$	R = 27.17 × $S_{wn}^{1.514}$
HU#2	33.1	0.085	0.754717	K = 42101φ3.3619	J = 0.085 × $S_{wn}^{-1.325}$	R = 77.88 × $S_{wn}^{1.325}$
HU#3	71.1	0.158	0.766284	K = 36714φ3.7966	J = 0.1587 × $S_{wn}^{-1.305}$	R = 108.00 × $S_{wn}^{1.305}$
HU#4	123.1	0.227	0.74184	K = 3275.1φ3.3917	J = 0.227 × $S_{wn}^{-1.348}$	R = 151.84 × $S_{wn}^{1.348}$
HU#5	220.8	0.2516	0.793651	K = 603.48φ3.5903	J = 0.2516 × $S_{wn}^{-1.26}$	R = 280.83 × $S_{wn}^{1.26}$

detailed relationships of porosity and permeability and combining with the obtained hydraulic flow units, the available capillary pressure curves can be divided into five categories. Figure 6 shows the five capillary pressure data sets for five hydraulic flow units. Following that, each of these capillary pressure curves is normalised into a single curve that represents hydraulic flow unit.

Figure 7 demonstrates J-function and normalised water saturation (S_{wn}) plotted along and presents the specific shape of one single capillary pressure curve for each hydraulic flow unit. When all parameters associated with the Equations 16 and 17 are computed, the water saturation for each hydraulic flow unit is calculated. Figure 8 illustrates examples of the matching result of water saturation between J-function and well log interpretation of reservoir rocks by dissimilar hydraulic flow units. This is a case study in which the method is applied for calculating water saturation in the reservoir, Cuu Long basin. Table 2 summarises all information including rock characteristics, lithology index, pore size distribution index, pore geometry constant, J-function and pore size radius equations observed for each hydraulic flow unit. Meanwhile, Table 3 demonstrates the comparison results of water saturation between the proposal approach and well log interpretation for all 18 wells in the field.

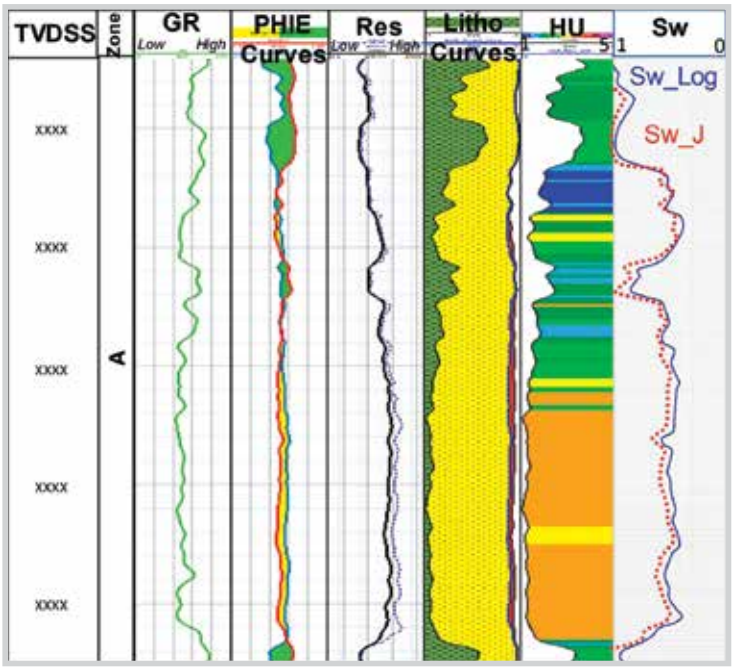

Figure 8. *Comparison results of water saturation between well log interpretation and J-function approach by dissimilar hydraulic flow units. The result is an example taken from Zone A at well 3.*

As the results in the Table 3, the tiny discrepancy from around 1% to 9%, the most-likely around 3% of water saturation between well log interpretation and the method - J-function application - illustrates the usefulness and applicability of this approach in future works.

6. Conclusions

The water saturation is determined by a new proposed technique. The flow zone indicator (FZI) approach is applied to separate the reservoir rock into five zones having similar rock characteristics,

Table 3. *Average water saturations by well log interpretation and J-function approach*

Well	Zones	Top MD	Bottom MD	Average S_w by J function approach	Average S_w from well log interpretation	Discrepancy (%)
1	A	XXXX	YYYY	0.38	0.406	6%
2	B	XXXX	YYYY	0.308	0.311	1%
3	A	XXXX	YYYY	0.25	0.238	-5%
4	B	XXXX	YYYY	0.21	0.207	-1%
5	A	XXXX	YYYY	0.374	0.38	2%
6	B	XXXX	YYYY	0.31	0.321	3%
7	A	XXXX	YYYY	0.45	0.441	-2%
8	B	XXXX	YYYY	0.422	0.4	-5%
9	A	XXXX	YYYY	0.418	0.426	2%
10	A	XXXX	YYYY	0.55	0.538	-2%
11	B	XXXX	YYYY	0.33	0.317	-4%
12	A	XXXX	YYYY	0.56	0.565	1%
13	B	XXXX	YYYY	0.35	0.339	-3%
14	A	XXXX	YYYY	0.588	0.579	-2%
15	B	XXXX	YYYY	0.22	0.242	9%
16	B	XXXX	YYYY	0.359	0.33	-9%
17	A	XXXX	YYYY	0.62	0.661	6%
18	B	XXXX	YYYY	0.26	0.245	-6%

which are considered as hydraulic flow units (HU). The measured capillary pressure curves are divided into five categories based on the determined hydraulic flow units. Then J-function is used to normalise all capillary curves that represent these flow units. The discrepancy of water saturation between well log interpretations and the proposal approach is inconsiderable.

Finally, the results indicated that the mentioned method is dependent on several rock properties and is not controlled to the specific reservoirs; it can be applied to any reservoir rocks having high heterogeneity in the future.

References

[1] M.C.Leverett, "Capillary behaviour in porous solids", *Transactions of the AIME*, Vol. 142, No. 1, pp. 152 - 169, 1941. DOI: 10.2118/941152-G.

[2] Ali Abedini and Farshid Torabi, "Pore size determination using normalized J-function for different hydraulic flow units", *Petroleum*, Vol. 1, No. 2, pp. 106 - 111, 2015.

[3] P.C.Carman, "Fluid flow through granular beds", *Chemical Engineering Research and Design*, Vol. 75, pp. 32 - 48, 1997. DOI: 10.1016/S0263-8762(97)80003-2.

[4] Ekwere J.Peters, *Advanced petrophysics: Dispersion, interfacial phenomena/wettability, capillarity/capillary pressure, relative permeability*. Live Oak Book Company, 2012.

[5] S.M.Desouky, "A new method for normalization of capillary pressure curves", *Oil & Gas Science and Technology*, Vol. 58, No. 5, pp. 551 - 556, 2003.